



# Unsteady mixed nano-bioconvection flow in a horizontal channel with its upper plate expanding or contracting



Ammarah Raees<sup>a</sup>, Hang Xu<sup>a,\*</sup>, Shi-Jun Liao<sup>a,b</sup>

<sup>a</sup>State Key Lab of Ocean Engineering, School of Naval Architecture, Ocean and Civil Engineering, Shanghai Jiao Tong University, Shanghai 200240, China

<sup>b</sup>Nonlinear Analysis and Applied Mathematics Research Group (NAAM), King Abdulaziz University (KAU), Jeddah, Saudi Arabia

## ARTICLE INFO

### Article history:

Received 9 June 2014

Received in revised form 18 February 2015

Accepted 1 March 2015

Available online 17 March 2015

### Keywords:

Unsteady flow

Bioconvection

Nanofluid

Gyrotactic microorganisms

## ABSTRACT

This article describes the unsteady flow of liquid containing nanoparticles and motile gyrotactic microorganisms between two parallel plates while keeping one moving and other fixed. The passively controlled nanofluid model is used to describe the nanoparticles concentration. Some instances of direct application of this nanofluid bioconvection study can be found in pharmaceutical industry, microfluidic devices, microbial enhanced oil recovery, modeling oil and gas-bearing sedimentary basins and many more. The governing partial differential equations are transformed to ordinary differential equations using the similarity transformations. The mathematica package based on homotopy analysis method is used to solve this problem. The physical phenomenon is explained by drawing the graphs for the temperature, nanoparticles concentration and density of motile microorganisms profiles. Also the tables are given which completely depicts the convergence of gained results.

© 2015 Elsevier Ltd. All rights reserved.

## 1. Introduction

The unsteady squeezing flow of a viscous fluid between parallel plates is of significant importance in the hydrodynamical machines, polymer processing, compression and injection moulding and lubrication equipment. Such type of flow is basically caused by the moving boundary under the influence of external normal stresses or vertical velocities. The earlier research work on squeezing flow by using the lubrication approximation was carried out by Stefan [1] and with the passage of time the researchers analyzed the squeezing flow in many different ways. Some numerical solutions of squeezing flow between parallel plates had been conducted by Verma [2] and later by Singh et al. [3]. Further, Hamza [4] had considered suction and injection effects on flow between plates reflecting squeezing flow. In addition to this the 2nd grade fluid flow between the rotating parallel plates was investigated in the papers by Rajagopal & Gupta [5] and Dandapat & Gupta [6]. Duwairi et al. [7] examined the effects of heat transfer on the squeezing flow of a viscous fluid. Khaled & Vafai [8] investigated the influence of magnetohydrodynamic effects on the squeezing flow and heat transfer over a sensor surface. Siddiqui et al. [9] analyzed the hydromagnetic squeezing flow of a viscous fluid between

parallel plates. Mustafa et al. [10] studied the heat and mass transfer in the unsteady squeezing flow between parallel plates. They also considered the dissipation effects and chemical reaction. Rashidi et al. [11,12] examined and solved the hydrodynamic squeezing flow of a viscous fluid and unsteady squeezing flow of a 2nd grade fluid between circular plates by homotopy analysis method.

The concept of enhancing the thermal conductivity of base fluids by adding the nanoparticles was first introduced by Choi [13]. After this a large number of research work and experiments were carried out to investigate the characteristics and heat transfer phenomenon in nanofluid such as Kakač and Pramuanjaroenkij [14], Wong and Leon [15], Saidur et al. [16], Wen et al. [17] and Buongiorno [18]. Ellahi et al. [19] considered the natural convection nanofluids flow along an inverted cone using Hamilton–Crosser model for the effective thermal conductivity. Ellahi [20] presented an analytical solution for a non-Newtonian nanofluid flow in a pipe with consideration of the effects of MHD and temperature dependent viscosity. Sheikholeslami et al. [21] studied the natural convection heat transfer in a nanofluid filled enclosure with elliptic inner cylinder. Ellahi et al. [22] made an analysis on non-Newtonian nanofluids flow through a porous medium between two coaxial cylinders with heat transfer and variable viscosity. Other important works relating to the theoretical and computational aspects can be found in Ellahi et al. [23], Akbar et al. [24], Sheikholeslami et al. [25], Sheikholeslami et al. [26],

\* Corresponding author.

E-mail addresses: [ammarah@sjtu.edu.cn](mailto:ammarah@sjtu.edu.cn), [ammarah\\_rafiqu@hotmail.com](mailto:ammarah_rafiqu@hotmail.com) (A. Raees), [hangxu@sjtu.edu.cn](mailto:hangxu@sjtu.edu.cn) (H. Xu), [sjliao@sjtu.edu.cn](mailto:sjliao@sjtu.edu.cn) (S.-J. Liao).

Akbar et al. [27]. Later on Kuznetsov and Nield [28] revised the Cheng–Minkowycz problem [29] by considering the passive boundary condition rather than active boundary condition. One of the most advancement in the heat transfer studies of nanofluid is the addition of microorganisms. Adding the microorganisms in base fluids such as algae and bacteria develops/generate the process of bioconvection [30] which is caused by their up swimming usually towards the source of light, gravity and oxygen and their density tends to be slightly higher than that of the ambient fluid, this can lead to an unstable density profile, with resultant overturning of the fluid. The suspension of microorganisms into nanofluids enhances its thermal conductivity significantly. The suspension of microorganisms in nanofluid was investigated in a series of papers published by Kuznetsov and Avramenko [31], Geng and Kuznetsov [32,33] and Kuznetsov [34–36]. Recently, Xu & Pop [37] examined the mixed convection flow in the horizontal channel filled by nanofluid containing both nanoparticles and gyrotactic microorganisms.

Several scientific problems are modeled by nonlinear ordinary or partial differential equations which can be solved by numerical and analytical techniques. Both of these techniques have some pros and cons. Numerical solutions can only be obtained for a set of discrete points on a curve which is often time consuming. Whereas analytical solutions are given at each point within the domain of interest. For this purpose researchers have been engaged in obtaining analytical solutions of various nonlinear problems in science and engineering. In this regard, the homotopy analysis method (HAM) proposed by Liao [38] in 1992 gives the analytic solutions for a variety of nonlinear problems. The new advancement in HAM is the development of a Mathematica package BVPh 2.0 [39] by Zhao & Liao. This analytic tool can be used to solve the system of linear/nonlinear ordinary differential equations. Moreover, the convergence of the results obtained by BVPh 2.0 is guaranteed by convergence-control parameter because it chooses the optimal value of convergence-control parameter at the minimum of squared residual at the desired order of approximation.

In this work, the unsteady squeezing flow of fluid containing both nanoparticles and gyrotactic microorganisms between the parallel plates is analyzed. Though in the literature survey, several aspects of nanofluid bioconvection has been presented but it still needs to be analyzed at fundamental level. So, it seems worthwhile attempt to compute the analytic solution for such an unsteady problem which is the extension of the work done by Kuznetsov [36]. Here in particular, we have considered passively controlled nanofluid model to formulate the problem and the fluid is considered between two parallel plates, one of which is moving and other is kept fixed. Also this is first such study in which the time-dependent mixed nano bioconvection flow has been investigated in a horizontal channel. Then the obtained governing nonlinear partial differential equations are transformed to nonlinear ordinary differential equations by using the similarity transformation and afterwards the problem is solved by applying the BVPh 2.0. Several aspects of the problem are investigated and shown graphically with respect to the physical parameters involved in it.

## 2. Mathematical formulation

Consider the unsteady two dimensional flow and heat transfer of an incompressible viscous fluid between two infinite parallel plates. The coordinate system is chosen such that the  $x$ -axis is along the lower plate and  $y$ -axis is normal to the plate, respectively as shown in Fig. 1. It is assumed that the two plates are placed at the distance  $y = h(t)$  while the upper plate is moving towards or away from the lower stationary plate with the velocity  $v(t) = dh/dt$ . It is also assumed that both plates are impermeable.

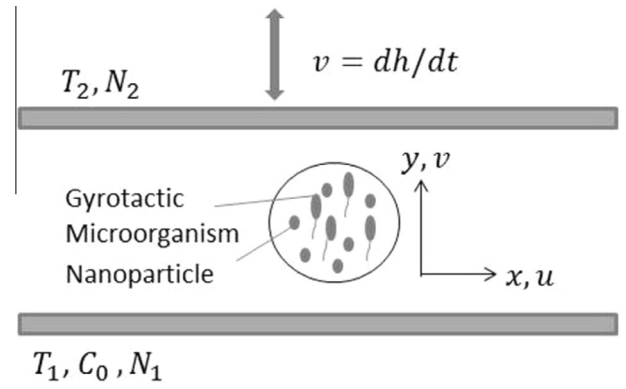


Fig. 1. The physical sketch and the coordinate system.

Further, it is assumed that the lower and upper plates are maintained at a constant temperature  $T_1$  and  $T_2$ , respectively. Here the symmetric nature of the flow is adopted. Also passively controlled nanofluid model is considered here and for this the upper plate has the passive boundary condition whereas at lower plate the nanoparticles distribution is a constant  $C_0$ . In addition to this, the distribution of microorganisms is also constant on lower and upper plates denoted as  $N_1$  and  $N_2$ . Here the base fluid is considered to be water because microorganisms can only survive in water. Together with this it is also assumed that the nanoparticles concentration is dilute and they do not agglomerate in the fluid. Under these assumptions and using nanofluid model proposed by [28], the governing conservation equations of mass, momentum, energy and mass transfer, nanoparticles volume fraction and microorganisms at unsteady state can be expressed as

$$\nabla \cdot \mathbf{v} = 0, \tag{1}$$

$$\rho_f \left( \frac{\partial \mathbf{v}}{\partial t} + \mathbf{v} \cdot \nabla \right) \cdot \mathbf{v} = -\nabla p + \mu \nabla^2 \mathbf{v}, \tag{2}$$

$$\frac{\partial T}{\partial t} + \mathbf{v} \cdot \nabla T = \alpha \nabla^2 T + \tau [D_B \nabla T \cdot \nabla C + (D_T/T_0) \nabla T \cdot \nabla T], \tag{3}$$

$$\frac{\partial C}{\partial t} + (\mathbf{v} \cdot \nabla) C = D_B \nabla^2 C + (D_T/T_0) \nabla^2 T, \tag{4}$$

$$\frac{\partial N}{\partial t} = -\nabla \cdot \mathbf{j}, \tag{5}$$

where  $\mathbf{v}$  is the velocity vector of the flow with  $u$  and  $v$  being the velocity components in  $x$ -direction and  $y$ -direction respectively,  $T$  is the temperature,  $C$  is the nanoparticle volumetric fraction,  $N$  is the number density of motile microorganisms,  $\mathbf{j}$  is the vector of the flux of microorganisms,  $p$  is the pressure,  $\rho_f$  is the density of nanofluid,  $\mu$  is the viscosity of the suspension of nanofluid and microorganisms,  $\alpha$  is the thermal diffusivity of the nanofluid,  $\tau = (\rho c)_p / (\rho c)_f$  is a parameter with  $(\rho c)_p$  being heat capacity of the nanoparticle and  $(\rho c)_f$  being the heat capacity of fluid,  $D_B$  is the Brownian diffusion coefficient,  $D_T$  is the thermophoretic diffusion coefficient,  $T_0$  is the reference temperature.

Following [36], the flux of microorganisms  $\mathbf{j}$  which is caused due to fluid convection, self-propelled swimming of microorganisms and diffusion of microorganism, is expanded as

$$\mathbf{j} = N\mathbf{v} + N\tilde{\mathbf{v}} - D_n \nabla N, \tag{6}$$

where  $D_n$  is the diffusivity of microorganisms,  $\tilde{\mathbf{v}}$  is the average swimming velocity vector of the oxytactic microorganism defined by

$$\tilde{\mathbf{v}} = (bW_c / \Delta C) \nabla C, \tag{7}$$

**Table 1**  
Error Analysis when  $h_f = h_\theta = h_\phi = h_s = -1$  for  $\beta = 3/2$  where  $w = 1, Pr = 1, Nt = Nb = 0.1, \delta_\theta = 1/2, \delta_\phi = 0, \delta_s = 1$ .

Order	$\epsilon_f$	$\epsilon_\theta$	$\epsilon_\phi$	$\epsilon_s$
2	16.1477	0.0003594	0.009128	0.02845
6	0.000155	$5.27037 \times 10^{-8}$	$2.42747 \times 10^{-6}$	$5.43077 \times 10^{-5}$
10	$3.95449 \times 10^{-9}$	$3.38701 \times 10^{-12}$	$2.45993 \times 10^{-10}$	$1.1147 \times 10^{-7}$
20	$5.46441 \times 10^{-20}$	$4.95039 \times 10^{-22}$	$2.33447 \times 10^{-20}$	$1.40039 \times 10^{-16}$
30	$1.57101 \times 10^{-31}$	$9.27053 \times 10^{-32}$	$3.60348 \times 10^{-30}$	$3.79339 \times 10^{-25}$

**Table 2**  
Error Analysis when  $h_f = h_\theta = h_\phi = h_s = -1$  for  $\beta = -3/2$  where  $w = 1, Pr = 1, Nt = Nb = 0.1, \delta_\theta = 1/2, \delta_\phi = 0, \delta_s = 1$ .

Order	$\epsilon_f$	$\epsilon_\theta$	$\epsilon_\phi$	$\epsilon_s$
2	278.036	0.00504677	0.261258	0.313662
6	$2.32217 \times 10^{-4}$	$7.36379 \times 10^{-7}$	$5.38212 \times 10^{-5}$	$1.59413 \times 10^{-2}$
10	$2.89185 \times 10^{-9}$	$1.94317 \times 10^{-10}$	$9.80332 \times 10^{-9}$	$2.61172 \times 10^{-5}$
20	$7.20342 \times 10^{-21}$	$3.32857 \times 10^{-19}$	$8.23022 \times 10^{-18}$	$3.71041 \times 10^{-12}$
30	$3.81939 \times 10^{-32}$	$7.37875 \times 10^{-28}$	$1.34633 \times 10^{-26}$	$6.72858 \times 10^{-19}$

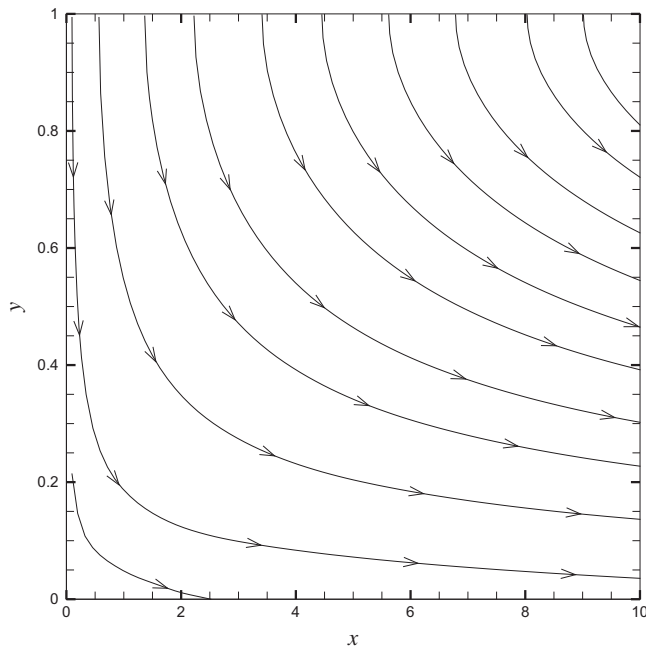


**Fig. 2.** Streamlines in the case of  $t = 0.1, w = 1, \beta = 1.5, Nt = Nb = 0.1, L_e = P_e = S_c = 1, Pr = 1$ .

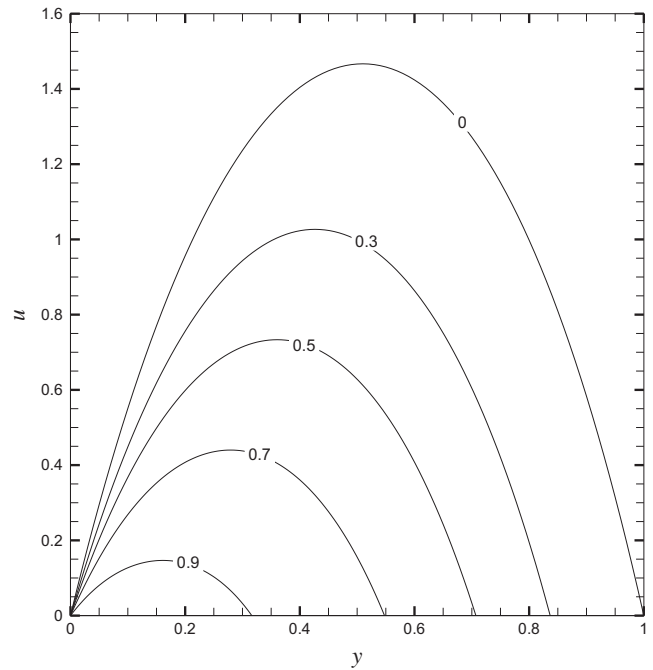


**Fig. 3.** Velocity component  $u$  in  $x$ -direction for different values of time  $t$  in the case of  $w = 1, \beta = 1.5, Nt = Nb = 0.1, L_e = P_e = S_c = 1, Pr = 1$ .

in which  $b$  is the chemotaxis constant and  $W_c$  is the maximum cell swimming speed relative to the nanofluid and is assumed to be constant. Applying the assumptions and doing simplifications to Eqs. (1)–(5) give rise to the following equations

$$\frac{\partial u}{\partial x} + \frac{\partial v}{\partial y} = 0, \tag{8}$$

$$\frac{\partial \xi}{\partial t} + u \frac{\partial \xi}{\partial x} + v \frac{\partial \xi}{\partial y} = v \left( \frac{\partial^2 \xi}{\partial x^2} + \frac{\partial^2 \xi}{\partial y^2} \right), \tag{9}$$

$$\frac{\partial T}{\partial t} + u \frac{\partial T}{\partial x} + v \frac{\partial T}{\partial y} = \alpha \left( \frac{\partial^2 T}{\partial x^2} + \frac{\partial^2 T}{\partial y^2} \right) + \tau D_B \left( \frac{\partial C}{\partial x} \frac{\partial T}{\partial x} + \frac{\partial C}{\partial y} \frac{\partial T}{\partial y} \right) + \frac{\tau D_T}{T_0} \left[ \left( \frac{\partial T}{\partial x} \right)^2 + \left( \frac{\partial T}{\partial y} \right)^2 \right], \tag{10}$$

$$\frac{\partial C}{\partial t} + u \frac{\partial C}{\partial x} + v \frac{\partial C}{\partial y} = D_B \left( \frac{\partial^2 C}{\partial x^2} + \frac{\partial^2 C}{\partial y^2} \right) + \frac{D_T}{T_0} \left( \frac{\partial^2 T}{\partial x^2} + \frac{\partial^2 T}{\partial y^2} \right), \tag{11}$$

$$\frac{\partial N}{\partial t} + u \frac{\partial N}{\partial x} + v \frac{\partial N}{\partial y} + \frac{\partial}{\partial y} (N\tilde{v}) = D_n \frac{\partial^2 N}{\partial y^2}, \tag{12}$$

where  $\xi = \frac{\partial v}{\partial x} - \frac{\partial u}{\partial y} = -\nabla^2 \psi$  and  $\tilde{v} = (bW_c/\Delta C) \frac{\partial C}{\partial y}$ . The appropriate initial and boundary conditions of Eqs. (8)–(12) is

$$\begin{aligned} u = 0, \quad v = \frac{dh}{dt}, \quad T = T_2, \quad D_B \frac{\partial C}{\partial y} + \frac{D_T}{T_0} \frac{\partial T}{\partial y} = 0, \quad N = N_2 \quad \text{at } y = h(t), \\ u = 0, \quad v = 0, \quad T = T_1, \quad C = C_0, \quad N = N_1 \quad \text{at } y = 0. \end{aligned} \tag{13}$$

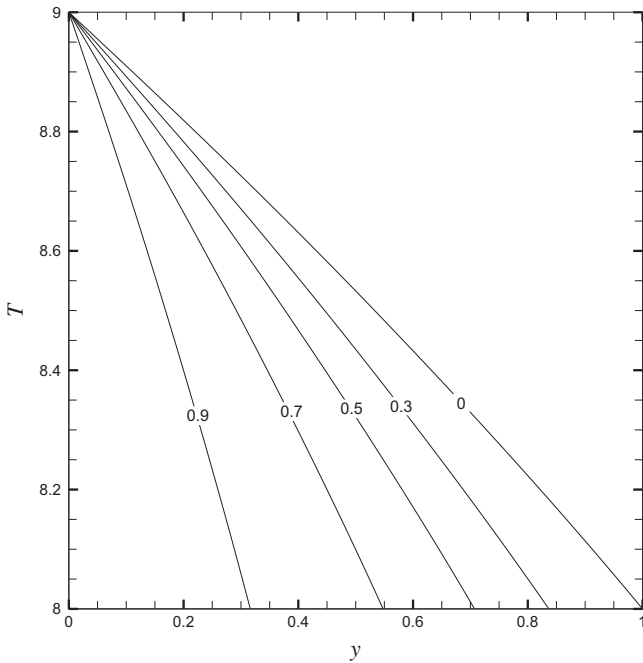


Fig. 4. Temperature  $T$  for different values of time  $t$  in the case of  $w = 1$ ,  $\beta = 1.5$ ,  $N_t = N_b = 0.1$ ,  $L_e = P_e = S_c = 1$ ,  $Pr = 1$ .

Now we introduce the following similarity transformations

$$\psi(x,y) = \left(\frac{bv}{1-\alpha t}\right)^{1/2} xf(\eta), \quad u = \frac{bx}{(1-\alpha t)} f'(\eta), \quad v = -\left(\frac{bv}{1-\alpha t}\right)^{1/2} f(\eta)$$

$$\eta = \left[\frac{b}{v(1-\alpha t)}\right]^{1/2} y, \quad \theta(\eta) = \frac{T-T_0}{T_2-T_0}, \quad \phi(\eta) = \frac{C-C_0}{C_0}, \quad s(\eta) = \frac{N-N_0}{N_2-N_0} \quad (14)$$

and substitute then to Eqs. (8)–(12) together with boundary conditions (13) generates the set of four ordinary differential equations

$$f'''' + ff'''' - f'f'' - \beta\eta f'''' - 3\beta f'' = 0, \quad (15)$$

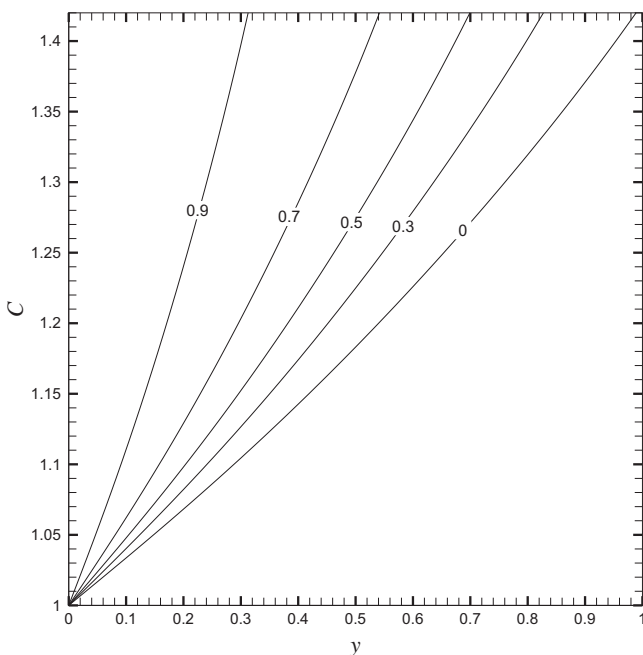


Fig. 5. Nanoparticle volumetric fraction  $C$  for different values of time  $t$  in the case of  $w = 1$ ,  $\beta = 1.5$ ,  $N_t = N_b = 0.1$ ,  $L_e = P_e = S_c = 1$ ,  $Pr = 1$ .

$$\theta'' + Pr(f\theta' - \beta\eta\theta') + N_b\theta'\phi' + N_t\theta^2 = 0, \quad (16)$$

$$\phi'' + L_e(f\phi' - \beta\eta\phi') + \frac{N_t}{N_b}\theta'' = 0, \quad (17)$$

$$s'' + S_c(fs' - \beta\eta s') - P_e\phi''s - P_e\phi's' = 0, \quad (18)$$

subject to following boundary conditions

$$f(0) = 0, \quad f'(0) = 0, \quad \theta(0) = 1, \quad N_b\phi'(0) + N_t\theta'(0) = 0, \quad s(0) = 1, \\ f'(1) = 0, \quad f(1) = w, \quad \theta(1) = \delta_\theta, \quad \phi(1) = \delta_\phi, \quad s(1) = \delta_s, \quad (19)$$

where

$$\beta = \frac{\alpha}{2b}, \quad Pr = \frac{\nu}{\alpha}, \quad N_b = \frac{\tau D_B C_0}{\alpha}, \quad N_t = \frac{\tau D_T (T_2 - T_0)}{T_0 \alpha}, \\ L_e = \frac{\nu}{D_B}, \quad P_e = \frac{b_c W_c}{D_n}, \quad S_c = \frac{\nu}{D_n}, \quad w = \frac{H\alpha}{2\sqrt{bv}}, \\ \delta_\theta = \frac{T_1 - T_0}{T_2 - T_0}, \quad \delta_\phi = \frac{C_1 - C_0}{C_0}, \quad \delta_s = \frac{N_1 - N_0}{N_2 - N_0}. \quad (20)$$

Here,  $\beta$  is the unsteadiness squeeze parameter where  $\beta > 0$  corresponds to the accelerating plates moving apart, while  $\beta < 0$  corresponds to the decelerating plates moving together (the so called squeezing flow), respectively. Also  $N_b$ ,  $N_t$ ,  $Pr$ ,  $L_e$ ,  $S_c$ , and  $P_e$  are respectively, the Brownian motion parameter, the thermophoresis parameter, the Prandtl number, the Lewis number, the Schmidt number, the bioconvection Peclet number and  $\delta_\theta$ ,  $\delta_\phi$ ,  $\delta_s$  and  $w$  are constants.

### 3. Solution method and error analysis

The nonlinear ordinary differential Eqs. (15)–(18) are solved by applying the BVP4c 2.0 [39]. This method is developed on the concept of computing with functions rather than numbers and this is why the singularities and infinite interval in the governing equations together with their boundary conditions are solved in a very easy way by using the computer algebra system such as Mathematica, Maple and so on. So in the frame of HAM it is reasonable to build such a Mathematica package which can be used

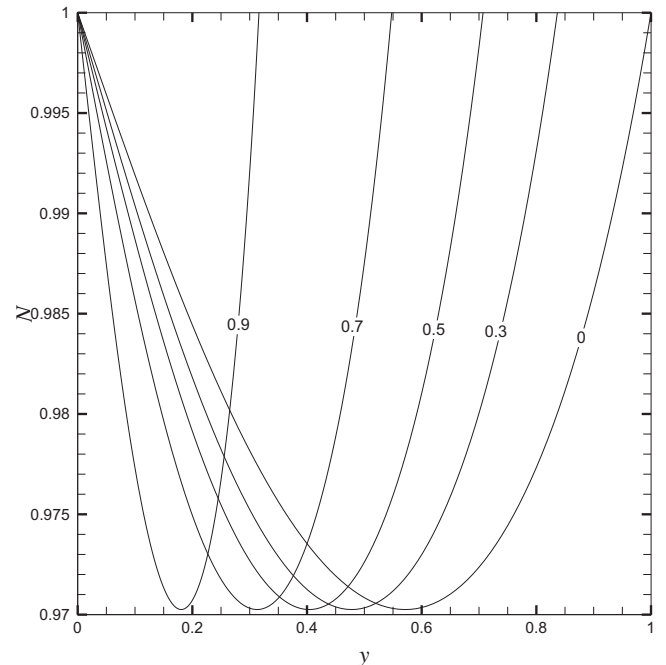


Fig. 6. Number density of motile microorganisms  $N$  for different values of time  $t$  in the case of  $w = 1$ ,  $\beta = 1.5$ ,  $N_t = N_b = 0.1$ ,  $L_e = P_e = S_c = 1$ ,  $Pr = 1$ .

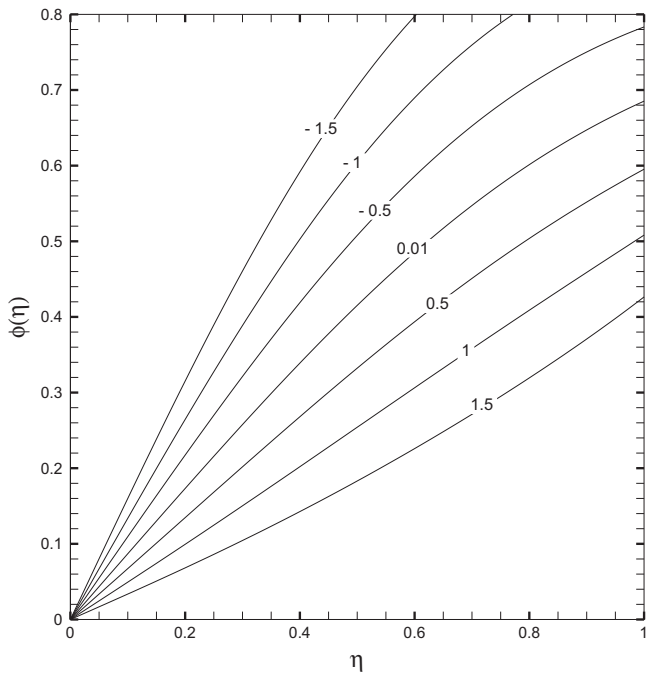


Fig. 7. Nanoparticle volume fraction profile  $s(\eta)$  for different values of squeeze parameter  $\beta$  in the case of  $w = 1$ ,  $N_t = N_b = 0.1$ ,  $L_e = P_e = S_c = Pr = 1$ .

efficiently to solve highly nonlinear ordinary differential equations with multiple solutions and singularities. BVP2.0 also has the potential to solve the system of nonlinear ordinary differential equations and eigenvalue problems in finite/semi-finite/infinite interval. As in HAM the convergence of obtained solution can be controlled by using the optimal value of the so called convergence-control parameter, which can be chosen at the minimum of squared residual of governing equations at certain order of approximations. In the similar manner, BVP2.0 guarantees the

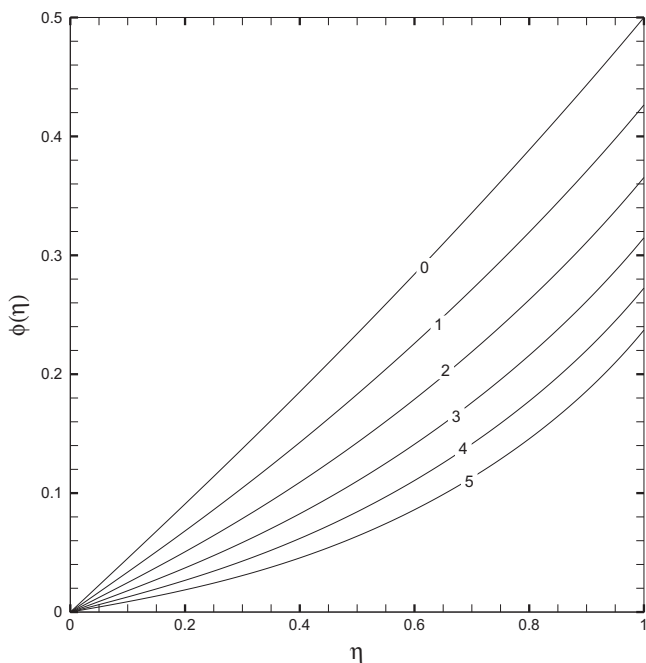


Fig. 8. Nanoparticle volume fraction profile  $s(\eta)$  for different values of  $L_e$  in the case of  $w = 1$ ,  $N_t = N_b = 0.1$ ,  $Pr = P_e = S_c = 1$ ,  $\beta = 1.5$ .

convergence of homotopy series by selecting the value of convergence-control parameter at the minimum error at some specified approximation. The error estimation functions for  $f(\eta)$ ,  $\theta(\eta)$ ,  $\phi(\eta)$  and  $s(\eta)$  in our calculations are defined as

$$\begin{aligned} \varepsilon_f &= \int_0^1 [f'''' + ff'''' - f'f'' - \beta\eta f'''' - 3\beta f''']^2 d\eta, \\ \varepsilon_\theta &= \int_0^1 [\theta'' + Pr(f\theta' - \beta\eta\theta') + N_b\theta'\phi' + N_t\theta'^2]^2 d\eta, \\ \varepsilon_\phi &= \int_0^1 [\phi'' + L_e(f\phi' - \beta\eta\phi') + \frac{N_t}{N_b}\theta'']^2 d\eta, \\ \varepsilon_s &= \int_0^1 [s'' + S_c(fs' - \beta\eta s') - P_e\phi''s - P_e\phi's']^2 d\eta. \end{aligned} \tag{21}$$

In addition to this, the convergence of homotopy series can be accelerated by using either the iteration approach or by applying the homotopy-pade approximations. Both of these techniques can also be employed to obtain the problem solution by directly using some simple commands. Further, the convergence of homotopy series also depends upon the selection of initial guess, the auxiliary linear operator and the auxiliary function. The chosen auxiliary linear operators for the current problem are as follows

$$L_f = \frac{\partial^4}{\partial \eta^4}, \quad L_\theta = L_\phi = L_s = \frac{\partial^2}{\partial \eta^2}, \tag{22}$$

whereas the initial guesses  $f_0(\eta)$ ,  $\theta_0(\eta)$ ,  $\phi_0(\eta)$  and  $s_0(\eta)$  are chosen based on the boundary conditions (19), which are given as

$$\begin{aligned} f_0(\eta) &= \frac{5w}{2}\eta^3 - \frac{3w}{2}\eta^5, \quad \theta_0(\eta) = 1 + (\delta_\theta - 1)\eta, \\ \phi_0(\eta) &= \delta_\phi + \left[\frac{N_t(1 - \delta_\theta)}{N_b}\right]\eta, \quad s_0(\eta) = 1 + (\delta_s - 1)\eta^3. \end{aligned} \tag{23}$$

Thus, BVP2.0 is applied successfully to solve the system of nonlinear ordinary differential Eqs. (15)–(18) subject to the boundary conditions (19). To ensure the convergence of our obtained results, the Tables 1 and 2 are presented in the case of  $\beta > 0$  and  $\beta < 0$ . Note that we have chosen  $\delta_\theta = 1/2$ ,  $\delta_\phi = 0$ ,  $\delta_s = 1$  and  $w = 1$  throughout

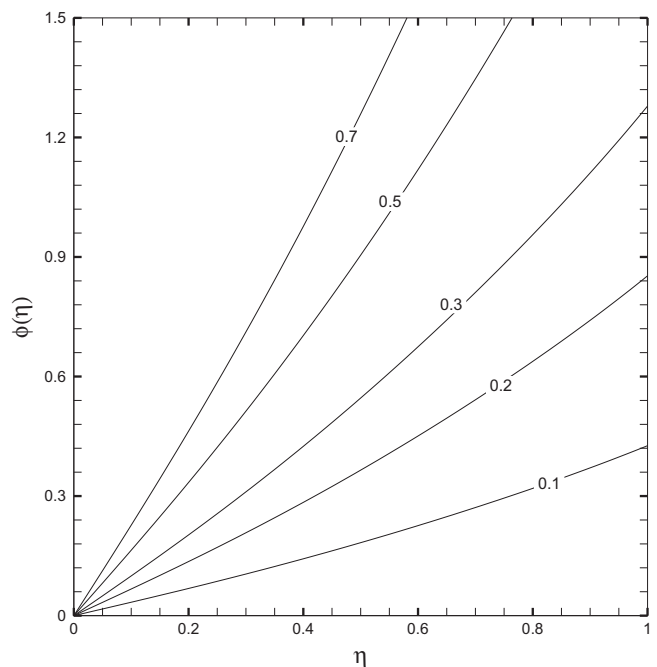
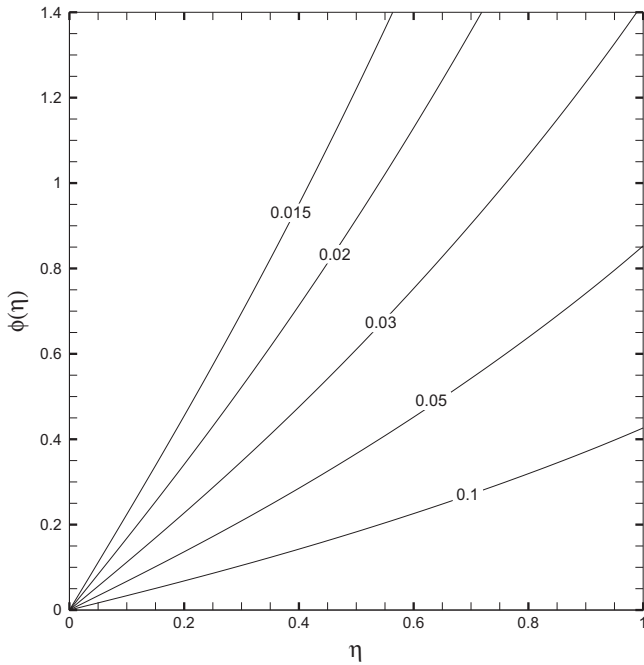


Fig. 9. Nanoparticle volume fraction profile  $s(\eta)$  for different values of  $N_t$  in the case of  $w = 1$ ,  $N_b = 0.1$ ,  $\beta = 1.5$ ,  $L_e = P_e = S_c = Pr = 1$ .



**Fig. 10.** Nanoparticle volume fraction profile  $s(\eta)$  for different values of  $N_b$  in the case of  $w = 1$ ,  $N_t = 0.1$ ,  $\beta = 1.5$ ,  $L_e = P_e = S_c = Pr = 1$ .

our calculations. Further, our computations shows that the obtained series solution converges when  $h_f = h_0 = h_\phi = h_s = -1$ . The reduction in the residual error with the increase in the order of approximations guarantees the convergence of resulting homotopy series.

**4. Results and discussion**

To get the better understanding of the physics of fluid flow, the streamlines at a given instant of time are shown in the Fig. 2. Here we have chosen  $t = 0.1$  and the case for  $\beta > 0$  is taken in account.

The dimensional velocity component and temperature are plotted at different values of time shown in Figs. 3 and 4. The figures shows that the velocity component decreases monotonously while the temperature decreases continuously as the time increases. Similarly, the nanoparticle volumetric fraction increases and number density of motile microorganisms decreases monotonously as the time increases as given in Figs. 5 and 6. Further, the addition of gyrotactic microorganisms in the nanofluid enhances its thermal conductivity. The combination of microorganisms and small particles make the nanofluid more stable because the settling of particles is slowed down and the mixing(mass transfer) is enhanced due to bioconvection [35]. Also the unstable density stratification at the upper fluid layer caused due to the upswimming of microorganism is compensated with the settling of small particles at the lower fluid layer.

Now we will discuss the effect of embedding physical parameters on the nanoparticles volume concentration  $\phi(\eta)$  and density of motile microorganisms  $s(\eta)$  profiles. For this purpose, the significant influence of the squeeze parameter  $\beta$ , the Lewis number  $L_e$ , the thermophoresis parameter  $N_t$ , the Brownian motion parameter  $N_b$  on nanoparticle volume fraction profile  $\phi(\eta)$  are displayed in Figs. 7–10. Fig. 7 depicts that the value of  $\phi(\eta)$  becomes greater and greater with the decreasing value of  $\beta$ . Here the values of  $\beta > 0$  is related to the upward motion of plate and  $\beta < 0$  corresponds to the downwards motion of upper plate towards the stationary lower plate. The variation of  $L_e$  on the  $\phi(\eta)$  is plotted in Fig. 8. It is observed from the figure that  $\phi(\eta)$  decreases continuously as the value of  $L_e$  evolves. Then the Figs. 9 and 10 shows the effects of  $N_t$  &  $N_b$  which illustrates the thermophoresis effect and Brownian motion on  $\phi(\eta)$ . Physically, Brownian motion can be observed due to the random motion of suspended nanoparticles, while thermophoresis effect is caused by the migration of nanoparticles due to the imposed temperature gradient across the fluid. The values of  $N_t$  &  $N_b$  signifies the thermophoresis effect and Brownian motion. So,  $N_t$  &  $N_b$  can be given any value in the range  $0 \leq N_t, N_b < \infty$ . It is noticed from Fig. 9 that increment in the value of  $N_t$  results in the enhancement of the value of nanoparticle volume fraction profile because increase in the  $N_t$  induced by

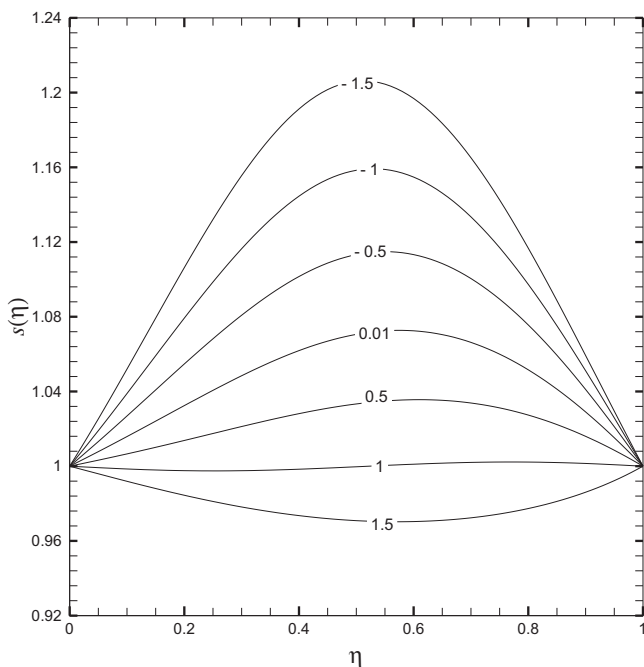


**Fig. 11.** Density of motile microorganisms profile  $s(\eta)$  for different values of squeeze parameter  $\beta$  in the case of  $w = 1$ ,  $N_t = N_b = 0.1$ ,  $L_e = P_e = S_c = Pr = 1$ .

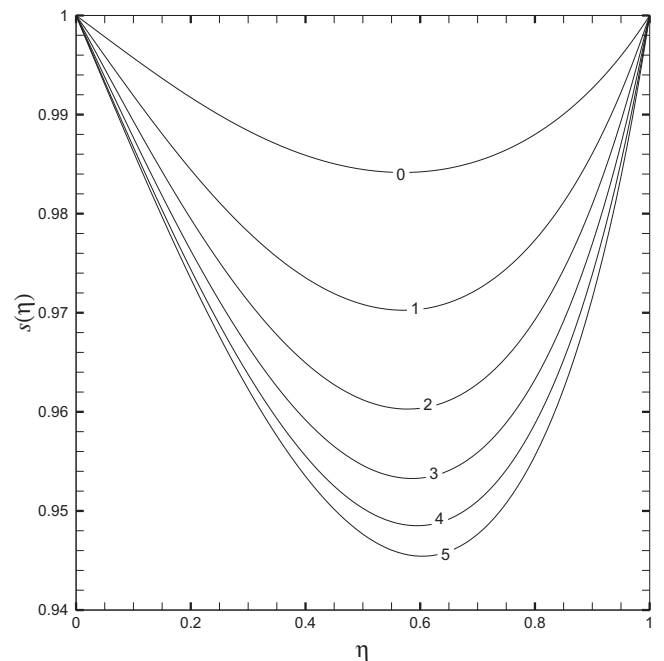


**Fig. 12.** Density of motile microorganisms profile  $s(\eta)$  for different values of  $L_e$  in the case of  $w = 1$ ,  $N_t = N_b = 0.1$ ,  $Pr = P_e = S_c = 1$ ,  $\beta = 1.5$ .

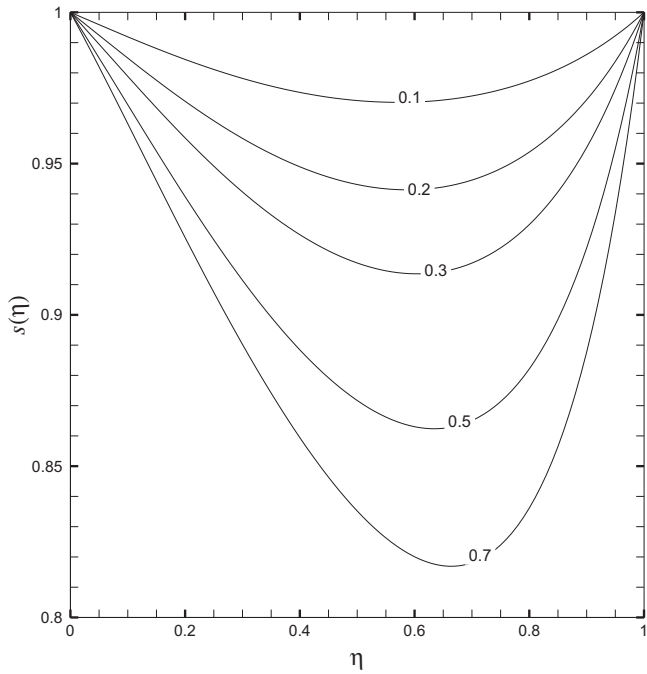


**Fig. 13.** Density of motile microorganisms profile  $s(\eta)$  for different values of  $N_t$  in the case of  $w = 1$ ,  $N_b = 0.1$ ,  $\beta = 1.5$ ,  $L_e = P_e = S_c = Pr = 1$ .

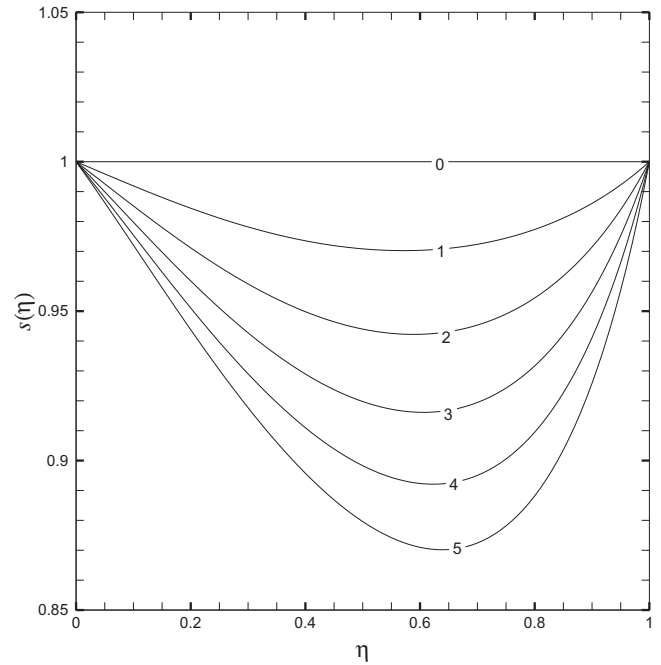


**Fig. 15.** Density of motile microorganisms profile  $s(\eta)$  for different values of  $P_e$  in the case of  $w = 1$ ,  $N_t = N_b = 0.1$ ,  $\beta = 1.5$ ,  $L_e = S_c = Pr = 1$ .

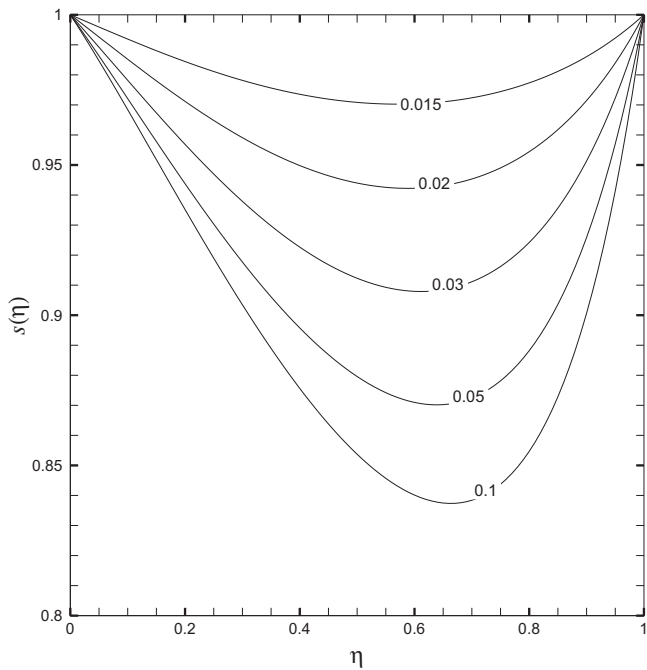


**Fig. 14.** Density of motile microorganisms profile  $s(\eta)$  for different values of  $N_b$  in the case of  $w = 1$ ,  $N_t = 0.1$ ,  $\beta = 1.5$ ,  $L_e = P_e = S_c = Pr = 1$ .

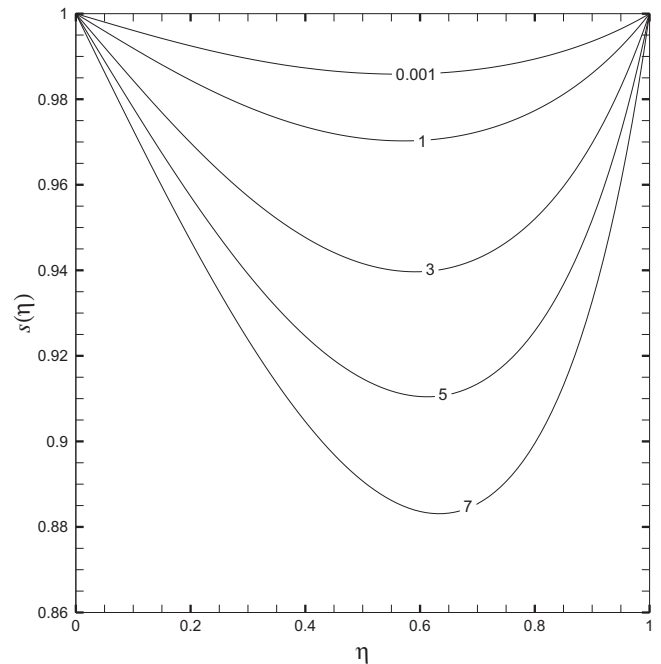


**Fig. 16.** Density of motile microorganisms profile  $s(\eta)$  for different values of  $Pr$  in the case of  $w = 1$ ,  $N_t = N_b = 0.1$ ,  $\beta = 1.5$ ,  $L_e = P_e = S_c = 1$ .

thermal gradient causes larger mass flux which results in rise of  $\phi(\eta)$ . But  $N_b$  behaves in an opposite manner on  $\phi(\eta)$  as compared to  $N_t$ . It is displayed in Fig. 10, that as the value of  $N_b$  becomes smaller and smaller the  $\phi(\eta)$  increases. It is worth mentioning here that nanoparticles volume concentration profile shows the deviation for the values of  $N_b$  ranging from  $0 \leq N_b \leq 2$  and it remains negligibly altered for the values of  $N_b > 2$ .

Figs. 11–16 are devoted to visualize the effect of density of motile microorganisms on the squeeze parameter  $\beta$ , the Levis

number  $L_e$ , the thermophoresis parameter  $N_t$ , the Brownian motion parameter  $N_b$ , the Prandtl number  $Pr$  and the bioconvection Peclet number  $P_e$ . The influence of squeeze parameter  $\beta$  on  $s(\eta)$  is presented in Fig. 11. It is noticed from the figure that initially  $s(\eta)$  increases gradually but as the  $\eta$  reaches the neighborhood of 0.6 it starts to decrease when the squeeze parameter is small. But as the value of  $\beta$  increases,  $s(\eta)$  shows an opposite trend because  $s(\eta)$  decreases firstly until  $\eta < 0.6$  and increases beyond this value of  $\eta$ . The variation of  $s(\eta)$  with other physical parameters

$Le$ ,  $N_t$ ,  $N_b$ ,  $Pr$  and  $Pe$  is quite similar to that of  $s(\eta)$  with  $\beta$ . As the value of Lewis number increases which describes the Brownian diffusion of nanoparticles, the density of motile microorganisms decreases for  $\eta < 0.6$  and increases after the 0.6 value of  $\eta$  as plotted in the Fig. 12. Similar to  $Le$ ,  $N_t$  and  $N_b$  shows the same trend on the  $s(\eta)$  as illustrated in Figs. 13 and 14. Finally, the effect of bioconvection Peclet number and Prandtl number on  $s(\eta)$  is given in Figs. 15 and 16. It is worth pointing here that as the microorganisms can survive only in water but for the computational ease we have chosen  $Pr = 1$  to gain all the graphical results and also our results are quite similar for  $Pr = 7$  and  $Pr = 1$ . The Prandtl number  $Pr = 0.72$ , 1.0 and 7.0 correspond to air, electrolyte solution, and water, respectively. In a liquid metal,  $Pr \ll 1$  and the energy diffusion rate greatly exceeds the momentum diffusion rate. The opposite is true for oils, for which  $Pr \gg 1$ .

## 5. Conclusions

In the present analysis, the investigation is made on the unsteady flow of nanofluid between parallel plates containing both nanoparticles and gyrotactic microorganisms. In particular, passively controlled nanofluid model is considered here to deeply understand the flow and heat transfer in the nanofluids. The governing physical problem is transformed to ordinary differential equations by using the similarity transformation. Then this problem is solved by using a newly developed Mathematica package BVPh 2.0 based on HAM. The gained analytic results for the mixed nano bioconvection time-dependent flow has not been reported before in literature. Some conclusions which we have drawn from our convergent results are as follows

- The convergent analytic solutions are obtained which are clear from the error analysis shown in the Tables 1 and 2.
- The non-dimensional velocity component, temperature, nanoparticle volume fraction and number density of motile microorganisms decreases with the increase in time.
- The nanoparticle volume fraction increases as the value of squeeze parameter decreases.
- The nanoparticles volume fraction decreases with an intensification in the Brownian motion effect but opposite trend is noticed in the case of thermophoretic effect.
- The density of motile microorganisms shows the monotonic behavior for the positive and negative values of squeeze parameter as well as for other parameters involved in problem.

## Conflict of interest

None declared.

## Acknowledgment

This work is supported by the Program for New Century Excellent Talents in University (Grant No. NCET-12-0347) and the authors are thankful for this support.

## References

- [1] M.J. Stefan, Versuch Über die scheinbare adhesion, Akademie der Wissenschaften in Wien. *Mathematik-Naturwissen* 69 (1874) 713.
- [2] R.L. Verma, A numerical solution for squeezing flow between parallel channels, *Wear* 72 (1) (1981) 89–95.
- [3] P. Singh, V. Radhakrishnan, K.A. Narayan, Squeezing flow between parallel plates, *Ingenieur-Archiv* 60 (4) (1990) 274–281.
- [4] E.A. Hamza, Suction and injection effects on a similar flow between parallel plates, *J. Phys. D: Appl. Phys.* 32 (6) (1999) 656–663.
- [5] K.R. Rajagopal, A.S. Gupta, On a class of exact solutions to the equations of motion of a second grade fluid, *Int. J. Eng. Sci.* 19 (7) (1981) 1009–1014.
- [6] B.S. Dandapat, A.S. Gupta, Stability of a thin layer of a second-grade fluid on a rotating disk, *Int. J. Non-Linear Mech.* 26 (3–4) (1991) 409–417.
- [7] H.M. Duwairi, B. Tashtoush, R.A. Damsheh, On heat transfer effects in a viscous fluid squeezed and extruded between two parallel plates, *Heat Mass Transfer* 41 (2004) 112–117.
- [8] A. Khaled, K. Vafai, Hydromagnetic squeezed flow and heat transfer over a sensor surface, *Int. J. Eng. Sci.* 42 (2009) 509–519.
- [9] A.M. Siddiqui, S. Irum, A.R. Ansari, Unsteady squeezing flow of a viscous MHD fluid between parallel plates, a solution using the homotopy perturbation method, *Math. Modell. Anal.* 13 (2008) 565–576.
- [10] M. Mustafa, T. Hayat, S. Obaidat, On heat and mass transfer in the unsteady squeezing flow between parallel plates, *Meccanica* 47 (2012) 1581–1589.
- [11] M.M. Rashidi, H. Shahmohammadi, S. Dinarvand, Analytic approximate solutions for unsteady two-dimensional and axisymmetric squeezing flows between parallel plates, *Math. Prob. Eng.* 2008 (2008) 13, <http://dx.doi.org/10.1155/2008/935095> (Article ID 935095).
- [12] M.M. Rashidi, A.M. Siddiqui, M. Asadi, Application of homotopy analysis method to the unsteady squeezing flow of a second-grade fluid between circular plates, *Math. Prob. Eng. vol. 2010* (2010) 18, <http://dx.doi.org/10.1155/2010/706840> (Article ID 706840).
- [13] S.U.S. Choi, Enhancing thermal conductivity of fluids with nanoparticle, in: *The Proceedings of the 1995 ASME International Mechanical Engineering Congress and Exposition*, ASME, FED 231/MD66, San Francisco, USA, 1995, pp. 99–105.
- [14] S. Kakač, A. Pramuanjaroenkij, Review of convective heat transfer enhancement with nanofluids, *Int. J. Heat Mass Transfer* 52 (2009) 3187–3196.
- [15] K.V. Wong, O.D. Leon, Applications of nanofluids: current and future, *Adv. Mech. Eng.* (2010) 11, <http://dx.doi.org/10.1155/2010/519659> (Article ID 519659).
- [16] R. Saidur, K.Y. Leong, H.A. Mohammad, A review on applications and challenges of nanofluids, *Renew. Sustainable Energy Rev.* 15 (2011) 1646–1668.
- [17] D. Wen, G. Lin, S. Vafaei, K. Zhang, Review of nanofluids for heat transfer applications, *Particuology* 7 (2011) 141–150.
- [18] J. Buongiorno, Convective transport in nanofluids, *J. Heat Transfer-Trans. ASME* 128 (3) (2006) 240–250.
- [19] R. Ellahi, M. Hassan, A. Zeeshan, Shape effects of nanosize particles in Cu – H<sub>2</sub>O nanofluid on entropy generation, *Int. J. Heat Mass Transfer* 81 (2015) 449–456.
- [20] R. Ellahi, The effects of MHD and temperature dependent viscosity on the flow of non-Newtonian nanofluid in a pipe: analytical solutions, *Appl. Math. Model.* 37 (3) (2013) 1451–1457.
- [21] M. Sheikholeslami, R. Ellahi, M. Hassan, S. Soleimani, A study of natural convection heat transfer in a nanofluid filled enclosure with elliptic inner cylinder, *Int. J. Numer. Methods Heat Fluid Flow* 24 (8) (2014) 1906–1927.
- [22] R. Ellahi, S. Aziz, A. Zeeshan, Non-Newtonian nanofluids flow through a porous medium between two coaxial cylinders with heat transfer and variable viscosity, *J. Porous Media* 16 (3) (2013) 205–216.
- [23] R. Ellahi, M. Raza, K. Vafai, Series solutions of non-Newtonian nanofluids with Reynolds' model and Vogel's model by means of the homotopy analysis method, *Math. Comput. Modell.* 55 (2012) 1876–1891.
- [24] N.S. Akbar, M. Raza, R. Ellahi, Influence of heat generation and heat flux in peristalsis with interaction of nanoparticles, *Eur. Phys. J.-Plus* 129 (185) (2014).
- [25] M. Sheikholeslami, R. Ellahi, H.R. Ashorynejad, G. Domairry, T. Hayat, Effects of heat transfer in flow of nanofluids over a permeable stretching wall in a porous medium, *Comput. Theor. Nanosci.* 11 (2) (2014) 486–496.
- [26] M. Sheikholeslami, M.G. Bandpy, R. Ellahi, A. Zeeshan, Simulation of CuO-water nanofluid flow and convective heat transfer considering Lorentz forces, *J. Magn. Magn. Mater.* 369 (2014) 69–80.
- [27] N.S. Akbar, S.U. Rahman, R. Ellahi, S. Nadeem, Nano fluid flow in tapering stenosed arteries with permeable walls, *Int. J. Thermal Sci.* 85 (2014) 54–61.
- [28] A.V. Kuznetsov, D.A. Nield, The Cheng–Minkowycz problem for natural convective boundary layer flow in a porous medium saturated by a nanofluid: a revised model, *Int. J. Heat Mass Transfer* 65 (2013) 682–685.
- [29] P. Cheng, W.J. Minkowycz, Free convection about a vertical flat plate embedded in a porous medium with application to heat transfer from a dike, *J. Geophys. Res.* 82 (14) (1977) 2040–2044.
- [30] T.J. Pedley, N.A. Hill, J.o. Kessler, The growth of bioconvection patterns in a uniform suspension of gyrotactic micro-organisms, *J. Fluid Mech.* 195 (1988) 223–237.
- [31] A.V. Kuznetsov, A.A. Avramenko, Effect of small particles on the stability of bioconvection in a suspension of gyrotactic microorganisms in a layer of finite depth, *Int. Commun. Heat Mass Transfer* 31 (2004) 1–10.
- [32] P. Geng, A.V. Kuznetsov, Effect of small solid particles on the development of bioconvection plumes, *Int. Commun. Heat Mass Transfer* 31 (2004) 629–638.
- [33] P. Geng, A.V. Kuznetsov, Introducing the concept of effective diffusivity to evaluate the effect of bioconvection on small solid particles, *Int. J. Transp. Phenom.* 7 (2005) 321–338.
- [34] A.V. Kuznetsov, The onset of bioconvection in a suspension of gyrotactic microorganisms in a fluid layer of finite depth heated from below, *Int. Commun. Heat Mass Transfer* 32 (2005) 574–582.
- [35] A.V. Kuznetsov, P. Geng, The interaction of bioconvection caused by gyrotactic micro-organisms and settling of small solid particles, *Int. J. Numer. Methods Heat Fluid Flow* 15 (2005) 328–347.

- [36] A.V. Kuznetsov, The onset of nanofluid bioconvection in a suspension containing both nanoparticles and gyrotactic microorganisms, *Int. Commun. Heat Mass Transfer* 37 (2010) 1421–1425.
- [37] H. Xu, I. Pop, Fully developed mixed convection flow in a horizontal channel filled by a nanofluid containing both nanoparticles and gyrotactic microorganisms, *Eur. J. Mech. B-Fluids* 46 (2014) 37–45.
- [38] S.J. Liao, The proposed homotopy analysis technique for the solution of nonlinear problems (Ph.D. thesis), Shanghai Jiao Tong University, 1992.
- [39] S.J. Liao, *Advances in the Homotopy Analysis Method*, World Scientific Publishing Co. Pte. Ltd., Singapore, 2014.